Age gap between the intrusion of gneissose granitoids and regional high-temperature metamorphism in the Ryoke belt (Mikawa area), central Japan

Kota Takatsuka[1], Tetsuo Kawakami[1,*], Etienne Skrzypek[1], Shuhei Sakata[1, 2], Hideyuki Obayashi[1], Takafumi Hirata[1,†]

Short running title: U−Pb zircon ages of Ryoke granitoids

[1]Department of Geology and Mineralogy, Graduate School of Science, Kyoto University, Kitashirakawa Oiwake-cho, Sakyo-ku, Kyoto 606-8502, Japan

[2]Department of Chemistry, Faculty of Science, Gakushuin University, 1-5-1 Mejiro, Toshima-ku, Tokyo 171-8588, Japan

*Corresponding author: T. Kawakami (e-mail: t-kawakami@kueps.kyoto-u.ac.jp)

[†]Present address: Geochemical Research Center, Graduate School of Science, The University of Tokyo, 7-3-1 Hongo, Bunkyo-ku, Tokyo 113-0033, Japan

ABSTRACT

The relationships between the intrusion of gneissose granitoids and the attainment of regional high-*T* conditions recorded in metamorphic rocks from the Ryoke belt of the Mikawa area, central Japan are explored. Seven gneissose granitoid samples (tonalite, granodiorite, granite) were collected from three distinct plutonic bodies that are mapped as the so-called "Older Ryoke granitoids." Based on bulk-rock compositions and U−Pb zircon ages obtained by laser ablation inductively coupled plasma mass spectrometry, the analyzed granitoids can be separated into two groups. Gneissose granitoids from the northern part of the area give weighted mean $^{206}Pb/^{238}U$ ages of 99 ±1 Ma (2 samples) and 95 ±1 Ma (1 sample), whereas those from the southern part yield 81 ±1 Ma (2 samples) and 78−77 ±1 Ma (2 samples). Regional comparisons allow correlating the northern granitoids (99−95 Ma) with the Kiyosaki granodiorite, and mostly with the Kamihara tonalite found to the east. The southern granitoids are tentatively renamed as "78−75 Ma (Hbl)−Bt granite" and "81−75 Ma Hbl−Bt tonalite", and seem to be broadly coeval members of the same magmatic suite. With respect to available age data, no gneissose granitoid from the Mikawa area shows a U−Pb zircon age which matches that of high-*T* metamorphism (*ca* 87 Ma). The southern gneissose granitoids (81−75 Ma), although they occur in the highest-grade metamorphic zone, do not seem to represent the

heat source which produced the metamorphic field gradient with a low dP/dT slope.

Key words: Gneissose granitoids, Heat source, LA-ICP-MS, Ryoke belt, U−Pb zircon dating,

1 INTRODUCTION

Low P/T type metamorphic belts are commonly characterized by abundant granitoids (e.g. De Yoreo, Lux, & Guidotti, 1991; Miyashiro, 1961), and these granitoids are often considered as one of the most important heat sources for high-T metamorphism (e.g. Lux et al., 1986). Some numerical modellings suggest that granitic intrusions can successfully explain the formation of the high-T conditions presently observed in the low P/T type metamorphic belts (Lux, De Yoreo, Guldotti, & Decker, 1986; De Yoreo, Lux, Guidotti, , Decker, & Osberg, 1989; De Yoreo et al., 1991; Okudaira, 1996). However, considering one or several plutons as the direct heat source of regional metamorphism requires that the age of plutonic activity coincides with that of high-T metamorphism. We explore this age relationship in the case of the Ryoke belt of central Japan.

Heat advection by plutons is considered to be a major process in the formation of regional metamorphic rocks in the Ryoke belt (e.g. Okudaira, 1996). Indeed, the belt is composed of abundant Late Cretaceous plutonic rocks occurring together with metamorphic rocks which record low-P, high-T metamorphic conditions on a regional scale (Miyashiro, 1961; Nakajima, 1994). The plutonic rocks have been classified into the Older and Younger Ryoke granitoids based on their structure and intrusive relationships (Hayama et al., 1982; Higashimoto, Nureki, Hara, Tsukuda, & Nakajima, 1983; Ryoke Research Group, 1972). The Older Ryoke granitoids show a gneissose structure which is concordant with the foliation of the host metamorphic rocks, whereas the Younger Ryoke granitoids are generally massive, discordantly cut the host-rock foliation, and create contact aureoles of variable widths.

The difference between the Older and Younger Ryoke granitoids is also one of thermal influence to the surrounding rocks. Until now, more importance has been given to the so-called Older Ryoke, i.e. gneissose granitoids. Gneissose granitoids generally occur within the highest-grade metamorphic zones and are regarded as syn-tectonic intrusions (Okudaira, Hara, Sakurai, & Hayasaka, 1993). In both the western (Yanai) and central (Mikawa) parts of the Ryoke belt (Figure 1), the similarity between chemical Th−U−total Pb isochron method (CHIME) monazite ages of high-grade pelitic gneisses (*ca* 100 Ma) and gneissose granitoids (*ca* 95 Ma) led to the interpretation that peak temperature conditions were contemporaneous with the emplacement of gneissose granitoids (Suzuki & Adachi, 1998). These structural and geochronological arguments were used to propose that heat advection by the gneissose granitoids produced high-T conditions on a regional scale (Harayama, Koido, Ishizawa, Nakai, & Kutsukake, 1985; Ikeda, 1998a; Okudaira, 1996; Okudaira et al., 1993; Okudaira & Suda, 2011).

However, an increasing number of U−Pb zircon ages obtained in granitoids from the Ryoke belt give a different view on the magmatic evolution (e.g. Iida et al., 2015; Nakajima, Kamiyama, Williams, & Tani, 2004; Skrzypek et al., 2016; Watanabe, Ireland, Tainosho, & Nakai, 2000). Sensitive high resolution ion microprobe (SHRIMP) U−Pb zircon dating of granitoids from the Kinki district reveals that gneissose granites are slightly younger than massive ones, suggesting that the gneissose character is not an appropriate criterion to infer the timing of granitoid intrusions (Watanabe et al., 2000). In addition, Murakami, Košler, Takagi, and Tagami (2006) report U−Pb zircon ages that differ from previous CHIME monazite ages (Miyake et al., 2016; Suzuki & Adachi, 1998) in the case of the Inagawa granite of the Mikawa area. More recently, Skrzypek et al. (2016) obtained U−Pb zircon ages older than CHIME monazite ages for granitoids in the Yanai area, and considered that U−Pb zircon ages better reflect the timing of granitoid intrusions. Indeed, rejuvenation of monazite is likely to have occurred during the intrusion of granitoids postdating the Ryoke regional metamorphism. In migmatite samples from the Aoyama area (Figure 1) monazite grains record two age populations ascribed to the timing of regional metamorphism and massive granite intrusion, respectively (Kawakami & Suzuki, 2011). The latter event is not recorded in zircon from the same area (Kawakami et al., 2013), suggesting that monazite is more easily rejuvenated than zircon during later thermal events. Based on these backgrounds, and considering that zircon is more robust than monazite against fluid-induced resetting (e.g. Bosse et al., 2009; Kawakami et al., 2014), it is necessary to use U−Pb zircon dating in order to re-evaluate the crystallization age of granitoids throughout the Ryoke belt.

In this study, we try to estimate the thermal influence of gneissose granitoids from the central part of the Ryoke belt (Mikawa area; Figure 1) where numerous CHIME monazite ages but scarce U−Pb zircon ages are available (e.g. Nakajima, 1996; Suzuki & Adachi, 1998). We report bulk-rock compositions and U−Pb zircon ages obtained by laser ablation inductively coupled plasma mass spectrometry (LA-ICP-MS) for gneissose (Older Ryoke) granitoids from the Mikawa area. We discuss the significance of U−Pb zircon ages and give possible causes for their discrepancy with CHIME monazite ages. With the help of existing geochemical and geochronological data, we lay the basis for the regional correlation of granitoid bodies in the Mikawa and Toyone areas (Figure 1) and discuss whether the presently exposed gneissose granitoids represent a plausible heat source of regional high-*T* metamorphism.

2 GEOLOGICAL SETTING AND PREVIOUS STUDIES

The Ryoke belt is located in the Inner Zone of southwest Japan and extends for about 800 km from northern Kyushu to Tsukuba (Figure 1). It records Cretaceous magmatic activity at the continental margin of East Asia; it is composed of abundant granitoids accompanied by low-P, high-T metamorphic rocks reaching granulite facies conditions (Brown, 1998; Ikeda, 1998a, 1998b, 2004; Kawakami, 2001; Miyashiro, 1961; Miyazaki, 2010; Nakajima, 1994; Okudaira et al., 1993). In central Japan, Ryoke metamorphic rocks surrounded by abundant granitoids are widely exposed in the Mikawa and Toyone areas (Figure 1).

2.1 Metamorphic rocks

The metamorphic rocks are thought to be derived from sediments of the Mino-Tamba accretionary complex (Wakita, 1987), and are composed of metachert, metasandstone and metamudstone with a small amount of metabasalt (Makimoto et al., 2004). The foliation of the metamorphic rocks strikes northeast−southwest to east−west and dips towards the north. The regional metamorphic grade increases from north to south across the biotite (Bt), K-feldspar−sillimanite (Kfs−Sil) and garnet−cordierite (Grt−Crd) zones (Miyazaki, Nishioka, Nakashima, & Ozaki, 2008; Nakashima, Hori, Miyazaki, & Nishioka, 2008; Figure 1). Contact metamorphic aureoles defined by the mineral assemblage Kfs + Crd (Kfs−Crd zone) are developed around the Younger Ryoke granitoids (Endo & Yamasaki, 2013; Miyazaki et al., 2008; Yamasaki & Ozaki, 2012).

Peak $P-T$ conditions are estimated to be 2.9−3.7 kbar/506−593 °C for the Bt zone, 3.7−4.3 kbar/574−709 °C for the Kfs−Sil zone, and 4.3−5.7 kbar/715−801 °C for the Grt−Crd zone (Miyazaki, 2010). Pressure−temperature estimates reported for the contact metamorphic aureole (Kfs−Crd zone) developed around the Shinshiro tonalite and Mitsuhashi granodiorite are 2.1−2.9 kbar/630−665 °C (Endo & Yamasaki, 2013).

Suzuki, Adachi, and Kajizuka (1994a) and Suzuki et al. (1994b) report CHIME monazite ages of 102−98 Ma for pelitic and psammitic gneisses from the Kfs−Crd zone. These CHIME monazite ages are thought to represent the timing of monazite growth at upper amphibolite facies conditions during regional metamorphism (e.g. Suzuki & Adachi, 1998). Nakajima et al. (2013) report SHRIMP U−Pb ages of *ca* 87 Ma for zircon grains belonging to both leucosomes and melanosomes of a migmatite sample from the Grt−Crd zone.

2.2 Plutonic rocks

Both the so-called Older and Younger Ryoke granitoids are exposed in the Mikawa and Toyone areas (Figure 1). The Older Ryoke granitoids include the Kamihara tonalite, Tenryukyo granite and Kiyosaki granodiorite, whereas the Younger Ryoke granitoids include the Shinshiro tonalite, Mitsuhashi granodiorite, Inagawa granite and Busetsu granite (Makimoto et al., 2004).

The Kamihara tonalite shows a gneissose structure and is mapped in northern and southern Mikawa as well as in Toyone (Figure 1). It has been considered as the oldest intrusion in these areas, and is intruded by the Tenryukyo granite, Mitsuhashi granodiorite and Busetsu granite (Ryoke Research Group, 1972). The main mineral assemblage is Pl + Qtz + Bt + Hbl with minor Kfs and cummingtonite (Kutsukake, 1993). Magmatic epidote is present in Kamihara tonalite samples from southern Mikawa while it is absent in those from northern Mikawa and Toyone, suggesting that the former record a deeper intrusion level than the latter (Masumoto, Enami, Tsuboi, & Hong, 2014). A tonalite sample from Toyone yields a CHIME monazite age of *ca* 95 Ma (Nakai & Suzuki, 1996).

The Tenryukyo granite shows a gneissose structure and is characterized by the presence of K-feldspar megacrysts up to 5 cm in length (Kutsukake, 1993). It is exposed in southern Mikawa and Toyone (Figure1), and is intruded by the Kiyosaki granodiorite, Mitsuhashi granodiorite and Inagawa granite (Ryoke Research Group, 1972). The Tenryukyo granite from southern Mikawa and Toyone shows CHIME monazite ages of *ca* 92−90 Ma (Nakai & Suzuki, 1996; Suzuki & Adachi, 1998).

The Kiyosaki granodiorite represents a small body (Figure 1) intruded by the Mitsuhashi granodiorite (Ryoke Research Group, 1972). The main facies is a locally diopside-bearing, Hbl−Bt granodiorite (Kutsukake, 2001). CHIME monazite ages of *ca* 87 Ma are reported from this granodiorite (Morishita et al., 1996), although the sampling locality is not published.

The Younger Ryoke granitoids range from tonalite to granite and yield CHIME monazite ages between 85 Ma and 75 Ma. The Shinshiro tonalite consists of a main facies of Hbl−Bt tonalite and a marginal facies of Bt tonalite and two-mica granite (Ohtomo, 1985). The marginal facies yielded CHIME monazite ages of *ca* 86−85 Ma (Morishita & Suzuki, 1995). The Mitsuhashi granodiorite mainly consists of Hbl−Bt tonalite and granodiorite (Kutsukake, 1997) with a CHIME monazite age of *ca* 84 Ma (Suzuki et al., 1994a, 1994b). The Inagawa granite is composed of Hbl−Bt granodiorite and Bt granite, and is subdivided into four petrographic types based on texture and modal abundance of biotite and hornblende (Nakai, 1974). A U −Pb zircon age of *ca* 73 Ma is reported for a sample collected within the Asuke shear zone which affects the southern part of the granite (Murakami et al., 2006). The Inagawa granite preserves CHIME monazite ages of *ca* 84−82 Ma (Miyake et al., 2016; Suzuki & Adachi, 1998). The Busetsu granite consists of four rock types: fine-grained Bt granodiorite, medium-grained Bt granite/granodiorite, medium-grained two-mica monzogranite and fine-grained two-mica granodiorite (Nakai & Suzuki, 2003). The Busetsu granite shows CHIME monazite ages of *ca* 79−75 Ma

(Nakai & Suzuki, 2003; Suzuki et al., 1994b;).

3 ANALYTICAL PROCEDURES

Fresh granitoid samples of about 250−800 g were collected at the localities indicated in Figure 1. Samples were cut into 2−3 cm-large cubes, reduced to about 80−110 g by quartering method, and powdered in an automated tungsten carbide mill following the method of Goto and Tatsumi (1994). Bulk-rock compositions were analyzed by ICP-ES and ICP-MS at Bureau Veritas Minerals Laboratories, Canada.

Granitoid samples from which zircon grains were separated were crushed using Selfrag at the National Institute of Polar Research (NIPR), Japan. Zircon grains were separated by panning followed by handpicking under a stereomicroscope, and mounted in epoxy. Cathodoluminescence (CL) and backscattered electron (BSE) images were acquired using a JEOL JXA-8105 superprobe at Kyoto University.

U−Pb zircon dating by LA-ICP-MS was done in Kyoto University and Gakushuin University. Age dating in Kyoto University was performed using a Nu PlasmaII multi-collector ICP-MS coupled to a NWR193 laser ablation system utilizing a 193 nm ArF excimer laser (10 µm spot diameter). Age dating in Gakushuin University was performed using an Agilent8800 single-collector ICP-MS coupled to a NWR213 laser-ablation system utilizing a 213 nm Nd:YAG laser (20 μm spot diameter). Zircon standard 91500 (Wiedenbeck et al., 1995, 2004) was used as a primary reference material for Pb/U and Th/U ratios while NIST SRM610 glass (Jochum & Brueckner, 2008; Pearce et al., 1997) was used for Pb/Pb ratios. Details on the analytical procedures and data reduction scheme are listed in Table S1, and the full dataset can be found in Table S2. Isoplot 4.15 (Ludwig, 2012) was used to construct concordia diagrams and to calculate weighted mean $^{206}Pb/^{238}U$ ages. Only analyses with concordance [= ($^{206}Pb/^{238}U$ age) $\times$ 100 / ($^{207}Pb/^{235}U$ age)] between 97 % and 103 % are referred to as concordant and are used for calculating weighted mean $^{206}Pb/^{238}U$ ages.

There are minor differences between secondary standard analyses obtained in the two laboratories when compared with recommended values. Analyses of secondary zircon standard GJ-1 yield a weighted mean $^{206}Pb/^{238}U$ age of 600.1 ±4.7 Ma (MSWD = 0.96, n = 22) in Kyoto University and 598.3 ±8.7 Ma (MSWD = 0.01, n = 3) in Gakushuin University, for a recommended value of 600.4 ±0.6 Ma? (weighted mean $^{206}Pb/^{238}U$ age using ID-TIMS analyses; Jackson, Pearson, Griffin, & Belousova, 2004). Analyses of secondary zircon standard from Plešovice yielded a weighted mean $^{206}Pb/^{238}U$ age of 342.9 ±3.3 Ma (MSWD = 0.47, n = 12) in Kyoto University and 338.5 ±4.9 Ma (MSWD = 0.26, n = 3) in Gakushuin University, for a recommended value of 337.13 ±0.37 Ma (weighted mean $^{206}Pb/^{238}U$ age using ID-TIMS analyses; Sláma et al., 2008). The observed variations can be attributed to the different apparatuses used and the small number of analytical sessions done at Gakushuin University. Although GJ-1 zircon analyses are in good agreement with the recommended value, analyses of the Plešovice zircon standard done at Kyoto University gave a slightly older age (1.7 %) than the recommended value. However, since this difference is small, we consider that inter-laboratory differences do not significantly bias our results.

4 SAMPLE DESCRIPTION

4.1 Gneissose granitoids in northern Mikawa

4.1.1 Samples GY88A and GY90A

Samples GY88A [N35.0371°, E137.3193°] and GY90A [N35.0177°, E137.3319°] are Hbl−Bt tonalites collected from northwest Mikawa (Figure 1). These samples belong to the pluton mapped as the Kamihara tonalite (e.g. Yamasaki & Ozaki, 2012) and show a weak to moderate gneissose structure defined by the arrangement of biotite and hornblende (Figure 2a,c). In both outcrops, the gneissose structure mostly strikes east−west and variably dips to the north, which is consistent with the foliation of metamorphic rocks in the Mikawa area. At the locality of GY88A, the gneissose structure does not show a consistent orientation and is locally cross-cut by quartz-rich leucocratic patches. Samples GY88A and GY90A mainly consist of Pl, Qtz, Kfs, Bt, and Hbl with accessory Ttn, Ilm, Ap, Aln, and Zrn (Figure 2b,d). Additionally, epidote is found overgrowing rims of allanite in sample GY88A. Minor clinopyroxene (Cpx) replaced by hornblende is present and epidote is absent in sample GY90A. Undulatory extinction of major constituting minerals points to solid-state deformation overprint in sample GY88A. In both samples, zircon is included in Qtz, Pl, Kfs, Bt and Hbl and also occurs along grain boundaries, and is included in allanite in sample GY90A (Figure 2b,d).

4.1.2 Sample GY98A

Sample GY98A [N35.0664°, E137.5417°] is a Cpx-bearing Hbl−Bt granodiorite collected from northeast Mikawa (Figure 1). This sample belongs to the pluton mapped as the Kiyosaki granodiorite (e.g. Makimoto et al., 2004), and shows a weak gneissose structure defined by the arrangement of biotite and hornblende (Figure 2e). Sample GY98A consists of Pl, Qtz, Kfs, Bt, Hbl, and Cpx with accessory Ttn, Py, Ap, and Zrn (Figure 2f), and secondary Chl. Clinopyroxene is partly replaced by hornblende. Zircon is included in Qtz, Pl and Bt, and also occurs along grain boundaries.

4.2 Gneissose granitoids in southern Mikawa

4.2.1 Sample GY33A

Sample GY33A [N34.8314°, E137.2777°] is a Hbl–Bt granite collected from southeast Mikawa (Figure 1). This sample belongs to the pluton mapped as the Kamihara tonalite (e.g. Miyazaki et al., 2008), and shows a pervasive gneissose structure defined by the arrangement of biotite and K-feldspar (Figure 3a,b). The sample appearance is close to that of an augen gneiss; the long axis of K-feldspar megacrysts (up to 3 cm in length) mostly lies parallel to the gneissose structure (Figure 3a), and the presence of quartz ribbons indicates an episode of solid-state ductile deformation. Metasandstone lenses (~ 5 cm thick, ~ 50 cm long) elongated parallel to the gneissose structure are common. The gneissose structure strikes east–west and dips to the north, which is consistent with the foliation of the surrounding metamorphic rocks. K-feldspar megacrysts define a weak, east–west trending, and subhorizontal mineral lineation. Sample GY33A mainly consist of Pl, Qtz, Kfs, Bt, and Hbl (Figure 3d), with accessory Aln, Ttn, Ep, Ap, Ilm, Py, Po, Zrn, and secondary Chl. Epidote is found as a matrix phase as well as overgrowth on allanite rims. Myrmekite is abundantly developed around K-feldspar. Zircon is included in Qtz, Pl, Kfs, Bt, and Aln, and also occurs along grain boundaries.

4.2.2 Sample GY48D

Sample GY48D [N34.8832°, E137.4424°] is a Bt granite collected from southeast

Mikawa (Figure 1). This sample belongs to a small body mapped as the Tenryukyo granite (Miyazaki et al., 2008), and shows a pervasive gneissose structure defined by the arrangement of biotite (Figure 3c). In the outcrop, the gneissose granite with rounded feldspars alternates with biotite- and sillimanite-bearing gneiss and leucocratic layers containing garnet and euhedral K-feldspar. The gneissose structure of the granite strikes east–west to northeast–southwest, dips to the north, and is consistent with the foliation of the neighboring metamorphic rocks. Sample GY48D is a fresh boulder with the same appearance as the nearby outcrop. It is weakly mylonitized, with plagioclase and K-feldspar grains wrapped by thin biotite. Constituent minerals are Pl, Qtz, Kfs, and Bt with accessory Aln, Ap, Zrn, and secondary Chl. Myrmekite is commonly developed around K-feldspar. Zircon is included in Qtz, Pl, Kfs, and Bt, and also occurs along grain boundaries (Figure 3e).

4.2.3 Samples GY80D and GY81B

Samples GY80D [N34.8011°, E137.1634°] and GY81B [N34.8008°, E137.1551°] are Hbl–Bt tonalites collected from southwest Mikawa (Figure 1). These samples belong to the pluton mapped as the Tenryukyo granite (e.g. Makimoto et al., 2004), and show a moderate gneissose structure defined by the alternation of leucocratic layers and aggregates of biotite and hornblende (Figure 3g,h). The gneissose structure strikes east–west and variably dips to the north, which is consistent with the foliation of metamorphic rocks in this area. In both outcrops, fine-grained Hbl-gabbro discordantly cuts the gneissose structure of the tonalite (Figure 3f). Both samples mainly consist of Pl, Qtz, Kfs, Bt, and Hbl, with accessory Aln, Ep, Ilm, Py, Po, Ttn, Ap, Zrn, and secondary Chl. Epidote is found as overgrowth on allanite rims. Zircon is included in Qtz, Pl, Bt, and Hbl, and also occurs along grain boundaries in both samples (Figure 3i,j). Allanite includes zircon in sample GY81B.

5 BULK-ROCK GEOCHEMISTRY

Bulk-rock analyses were performed for all samples except for sample GY98A and weathered sample GY90A. The results are summarized in Table 1 and plotted in Figure 4, together with data from previous studies of the Kamihara tonalite and Tenryukyo granite (Ishihara & Chappell, 2007; Ishihara & Terashima, 1977; Kutsukake, 1993; Masumoto et al., 2014; Morishita & Suzuki, 1993; Nakai, 1976; Tsuboi & Asahara, 2009; Yamasaki, 2013).

Data from previous studies show a clear difference between the Tenryukyo and Kamihara granitoid samples (Figure 4). The SiO_2 content of the Tenryukyo granite (> 67.9 wt%) is higher than that of the Kamihara tonalite (< 67.7 wt%). Among analyses of the Kamihara tonalite, samples from Toyone and northern Mikawa ('Northern' in Figure 4) show nearly similar compositions, whereas samples from southwest Mikawa show slightly lower SiO_2 and higher Al_2O_3 contents (Figure 4).

Sample GY88A from northern Mikawa is relatively rich in MgO content (3.8 wt%) with a SiO_2 content of 59.5 wt%; its composition is consistent with that of the Kamihara tonalite, especially with analyses previously reported from Toyone and northern Mikawa (Figure 4). Samples GY33A and GY48D from southeast Mikawa are characterized by high SiO_2 (60.8−64.7 wt%) and K_2O contents (3.5−4.7 wt%). The high K_2O content, especially in sample GY33A, is explained by the presence of K-feldspar megacrysts (Figure 3a,b). The composition of both samples falls in the range of the Tenryukyo granite, except for sample GY33A in the SiO_2 vs. K_2O diagram (Figure 4c). The composition of samples GY80D and GY81B from southwest Mikawa always falls outside the field defined by previous analyses of the Kamihara tonalite (Figure 4a−d). For similar SiO_2 contents, samples GY80D and GY81B show slightly lower K_2O (1.1−1.4 wt%) and markedly lower MgO (1.3−1.5 wt%) contents than published analyses of the Kamihara tonalite from Toyone and northern Mikawa (Figure 4a−c).

Among trace elements, Zr helps to distinguish between samples. Sample GY88A has a low Zr content (155 ppm) which agrees with previous analyses of the Kamihara tonalite from both Toyone and northern Mikawa, while samples GY33A and GY48D (163−185 ppm) are consistent with analyses reported for the Tenryukyo granite (Figure 4d). On the other hand, samples GY80D and GY81B are characterized by remarkably high Zr contents (356−361 ppm) which clearly differ from any previous analyses of gneissose granitoids in the Mikawa and Toyone areas (Figure 4d).

6 U−PB ZIRCON DATING

Cathodoluminescence images of representative zircon grains from all granitoid samples are presented in Figure 5. The three samples from northern Mikawa (GY88A, GY90A, GY98A) show zircon grains with oscillatory- or sector-zoned cores surrounded by oscillatory-zoned rims that discontinuously overgrow cores (Figure 5). Samples from southeast Mikawa (GY33A, GY48D) preserve zircon grains with oscillatory-zoned or homogeneous cores surrounded by oscillatory-zoned rims that discontinuously overgrow cores, while those from southwest Mikawa (GY80D, GY81B) show zircon grains with dark oscillatory- or sector-zoned cores, surrounded by bright oscillatory-zoned or homogeneous rims (Figure 5).

6.1 Gneissose granitoids in northern Mikawa

6.1.1 Sample GY88A

A total of 33 spots was obtained on 12 grains (spots 36.1−38.7; Table S2). Three analyses were rejected because of irregular signals. Concordant $^{206}Pb/^{238}U$ ages obtained from 25 analyses range from 105 Ma to 96 Ma, and their weighted mean is 98.9 ±0.9 Ma (25 spots, MSWD = 0.67; Figure 6a).

6.1.2 Sample GY90A

A total of 32 spots was obtained on 13 grains (spots 38.8−40.13; Table S2). Two grains preserve inherited cores with $^{207}Pb/^{206}Pb$ ages of *ca* 2450 Ma and *ca* 2040 Ma. Concordant $^{206}Pb/^{238}U$ ages obtained from 27 analyses range from 103 Ma to 96 Ma, and their weighted mean is 99.4 ±0.9 Ma (27 spots, MSWD = 0.44, Figure 6b).

6.1.3 Sample GY98A

A total of 32 spots was obtained on 15 grains (spots 66.8−68.13; Table S2). One grain shows inherited core and mantle parts with $^{207}Pb/^{206}Pb$ ages of *ca* 2120 Ma and *ca* 1800 Ma, respectively. Concordant $^{206}Pb/^{238}U$ ages obtained from 19 analyses range from 97 Ma to 91 Ma, and their weighted mean is 94.7 ±0.7 Ma (19 spots, MSWD = 1.4; Figure 6c).

6.2 Gneissose granitoids in southern Mikawa

6.2.1 Sample GY33A

A total of 76 spots was obtained on 35 grains (spots 2.12−4.10 and 23.1−27.7; Table S2). Seven analyses were rejected because of irregular signals. One zircon rim analysis was also rejected because it gave an older age than the core part of the same grain (spot 24.12; Table S2). One grain shows a CL-bright, inherited core with a $^{207}Pb/^{206}Pb$ age of *ca* 1790 Ma. Concordant $^{206}Pb/^{238}U$ ages obtained form 45 analyses range from 81 Ma to 74 Ma, and their weighted mean is 77.6 ±0.6 Ma (45 spots, MSWD = 2.3; Figure 6d).

6.2.2 Sample GY48D

A total of 52 spots was obtained on 31 grains (spots 7.1−8.13 and 21.1−22.13; Table S2). Concordant $^{206}Pb/^{238}U$ ages obtained from 37 analyses range from 82 Ma to 74 Ma, and their weighted mean is 77.1 ±0.6 Ma (37 spots, MSWD = 1.2; Figure 6e).

6.2.3 Sample GY80D

A total of 33 spots was obtained on 12 grains (spots 28.1−30.7; Table S2). Five analyses were rejected because of irregular signals. One grain preserves an inherited core with a $^{207}Pb/^{206}Pb$ age of 2501 ±20 Ma. Concordant $^{206}Pb/^{238}U$ ages obtained from 15 analyses range from 84 Ma to 78 Ma, and their weighted mean is 81.1 ±1.0 Ma (15 spots, MSWD = 0.62; Figure 6f).

6.2.4 Sample GY81B

A total of 32 spots was obtained on 12 grains (spots 30.8−32.13; Table S2). Four analyses were rejected because of irregular signals. Concordant $^{206}Pb/^{238}U$ ages obtained from 14 analyses range from 84 Ma to 79 Ma, and their weighted mean is 81.1 ±1.0 Ma (14 spots, MSWD = 0.64; Figure 6g).

7 DISCUSSION

7.1 Significance of U−Pb zircon ages

In all granitoid samples, zircon occurs along grain boundaries or as inclusion in the various major minerals (Figures 2 and 3). Most zircon grains show oscillatory- or sector-zoning patterns and do not contain older, inherited core parts (Figure 5). For each sample, U−Pb data obtained from both core and rim parts define a single age population (Figures 5 and 6). Therefore, the weighted mean $^{206}Pb/^{238}U$ zircon ages calculated with concordant analyses are interpreted to represent the timing of zircon crystallization from melt. We consider that this approximates the timing when granitoids were at their final emplacement depths.

An important feature of our samples is that they are deformed granitoids, as suggested by the clear solid-state overprints observed in samples GY33A, GY48D, and GY88A (Figure 3d,e). Wayne and Sinha (1988) observed that zircon grains from a mylonitic shear zone undergo grain size reduction, fracturing and Pb loss. In our samples, zircon does not show deformation features such as undulatory extinction. In addition, we avoided zircon grains showing micro-cracks or potential zones of secondary alteration for U−Pb analysis. The concordia diagrams document no significant Pb loss, discordant analyses being rather the result of mixing with a common Pb component (Figure 6). We therefore consider that the observed deformation had no influence on the U−Pb system in zircon, and that all ages are of primary magmatic origin.

U−Pb zircon ages give new constraints on the magmatic history of the Ryoke belt in the Mikawa area. The oldest granitoids occurring in northern Mikawa were emplaced in the period from *ca* 99 Ma to *ca* 95 Ma (Figure 7). Within the northern granitoids, our data show that there is small age gap between rocks located to the west (Kamihara tonalite samples GY88A, GY90A) and those located to the east (Kiyosaki granodiorite sample GY98A). Granitoids from southern Mikawa area show distinctly younger ages; consistent data from two pairs of samples indicate granitoid emplacement at c*a* 81 Ma (southwest Mikawa) and *ca* 78−77 Ma (southeast Mikawa).

In the case of granitoids from southwest Mikawa, we observe a discrepancy between U−Pb zircon ages and previous CHIME monazite ages (Figure 7). Samples GY80D and GY81B yield weighted mean $^{206}Pb/^{238}U$ zircon ages of 81 ±1.0 Ma, whereas a CHIME monazite age of 92.2 ±6.0 Ma is reported for a sample from the same pluton (Suzuki & Adachi, 1998). In granitoids from the western part of the Ryoke belt (Yanai area), Skrzypek et al. (2016) found that U−Pb zircon ages are systematically older than CHIME monazite ages. This kind of discrepancy can be expected if monazite is considered less robust than zircon and more prone to isotopic resetting during hydrothermal alteration of granites (e.g. Poitrasson, Chenery, & Bland, 1996).

In the present case, however, U−Pb zircon ages are younger than CHIME monazite results. This could be due to the difference between the samples dated in this study and that analyzed by Suzuki and Adachi (1998). Our samples except GY48D were collected from 30−3000 m away from pelitic gneiss; they contain allanite but no monazite is found, which is in agreement with the description of the main granitoid facies in southwest Mikawa (Masumoto et al., 2014). Conversely, the sample analyzed by Suzuki and Adachi (1998) is a leucocratic biotite granite which occurs at the margin of the pluton; it is in contact with pelitic gneiss and contains monazite. Based on the presence of monazite in this marginal facies, we cannot exclude the possible assimilation of material from the surrounding metasediments in which older monazite grains might be present. Indeed, in the northern part of the Mikawa area, monazites with CHIME age domains of 99 ±6−11 Ma are found in metasedimentary rocks (Suzuki et al., 1994a, 1994b). Therefore, we consider that zircon should be preferred to monazite when trying to assess the crystallization age of the main facies of allanite-bearing granitoids.

7.2 Regional correlation of granitoids in the Mikawa and Toyone areas

Gneissose granitoids from the Mikawa area were originally divided into two major plutons: the Kamihara tonalite and the Tenryukyo granite (Figure 1). This classification is actually based on lithological similarities with type localities that occur outside the Mikawa area (e.g. Makimoto et al., 2004). However, we illustrate that gneissose granitoid samples formerly classified as the same pluton are different not only in lithology, but also in bulk-rock composition and U−Pb zircon age (Figures 2−6). Even if we accept lithological variety within a single pluton, our results indicate that correlating different gneissose granitoids should take into account a more comprehensive dataset, especially U−Pb zircon ages.

For granitoids from northern Mikawa, the bulk-rock composition of sample GY88A agrees with previous analyses from the same pluton (Ishihara & Chappell, 2007; Ishihara & Terashima, 1977; Morishita & Suzuki, 1993; Nakai, 1976; Tsuboi & Asahara, 2009; Yamasaki, 2013; Figure 4). It is also compatible with bulk-rock data from Toyone (Kutsukake, 1993; Tsuboi & Asahara, 2009; Figure 4), which is the type locality of the

Kamihara tonalite (Sakakibara, 1967). Two samples (GY88A, GY90A) from northern Mikawa yield U−Pb zircon ages of 99 ±1 Ma which are close to the SHRIMP U−Pb zircon age of 96 ±1 Ma obtained from the type locality of the Kamihara tonalite (Figure 7; Tani, Horie, Dunkley, & Ishihara, 2014). All these similarities suggest that the gneissose tonalite exposed in northern Mikawa can be correlated with the Kamihara tonalite of Toyone (Figure 8).

For granitoids from southeast Mikawa, samples GY33A and GY48D mapped respectively as "Kamihara tonalite" and "Tenryukyo granite" (Miyazaki et al., 2008) show a pervasive gneissose structure and K-feldspar megacrysts (Figure 2), i.e. lithological features that are described for granitic rocks mapped as the "Tenryukyo granite" in Toyone (Kutsukake, 1993). Both samples are K_2O-rich granite with bulk-rock compositions that match those reported for the "Tenryukyo granite" exposed in Toyone (Kutsukake, 1993; Figure 4). In addition, they yield U−Pb zircon ages of 78 ±1 to 77 ±1 Ma which are consistent with the SHRIMP U−Pb zircon age of a "Tenryukyo granite" sample from Toyone (75 Ma; Tani et al., 2014). All these lithological, geochemical and geochronological similarities suggest that granitic rocks from southeast Mikawa and those mapped as "Tenryukyo granite" in Toyone can be regarded as the same pluton (Figure 8). However, the absence of comprehensive data, especially U−Pb zircon ages, for the actual type locality of the Tenryukyo granite (Yasuoka village, Nagano prefecture; Koide, 1942) precludes from using the name "Tenryukyo granite". Instead, we tentatively group the granites from southeast Mikawa and Toyone under the term "78−75 Ma (Hbl)−Bt granite" (Figure 8).

Samples GY80D and GY81B from southwest Mikawa, mapped as "Tenryukyo granite" (Makimoto et al., 2004), show numerous similarities. Both are Hbl−Bt tonalites with analogous bulk-rock compositions and identical U−Pb zircon ages of 81 ±1 Ma (Figures 4 and 6). One sample from a nearby small body mapped as "Kamihara tonalite" gave a U−Pb zircon age of *ca* 75 Ma (Figure 7; Tani et al., 2014). Judging from these results, we question the actual presence of different plutons in southwest Mikawa, and tentatively group all rocks of tonalitic composition in southwest Mikawa under the term "81−75 Ma Hbl−Bt tonalite" (Figure 8).

To summarize, gneissose granitoids from northern Mikawa can be correlated with rocks of similar age and composition in the Toyone area; the dominant facies can be called Kamihara tonalite (Figure 8). Gneissose granitoids from southern Mikawa are subdivided into the newly defined "81−75 Ma Hbl−Bt tonalite" and "78−75 Ma (Hbl)−Bt granite" groups. When previous analyses of the granite mapped as "Tenryukyo granite" in Toyone and southwest Mikawa granitoids are considered together with those of samples GY80D, GY81B, GY33A, and GY48D, a possible trend of decreasing MgO and Zr with increasing SiO_2 can be observed (Figure 4). This suggests that, in addition to overlapping U−Pb zircon ages (Figure 7), the "81−75 Ma" and "78−75 Ma" granitoids might preserve the same compositional trend related to magmatic differentiation. In such a case, the age similarity is a powerful argument to group both plutons while the difference in composition does not rule out a common origin.

7.3 Relationships between gneissose granitoids and regional high-*T* metamorphism

In the Ryoke belt, the presence of high-*T* conditions on a regional scale is deduced from the succession of wide metamorphic zones that define a low d*P*/d*T* metamorphic field gradient (e.g. Miyashiro, 1961; Figure 1). In the Mikawa area, the highest grade Grt−Crd zone is exposed in the southern part and hosts migmatite from which a SHRIMP U−Pb zircon age of *ca* 87 Ma is reported (Nakajima et al., 2013; Figure 7). In detail, the age of ca. 87 Ma was obtained from the rim of zircon grains located in both the leucosome and melanosome parts of a migmatite sample. Nakajima et al. (2013) considered these zircon rims as overgrowths formed during anatexis and interpreted the age as that of regional metamorphism. In a similar migmatite from the Grt−Crd zone of the Aoyama area (Figure 1), Kawakami et al. (2013) report melt inclusions in zircon rims and proposed that such rims formed at suprasolidus conditions and record the age of near-peak to early retrograde metamorphism. Therefore, we regard the *ca* 87 Ma age (Nakajima et al., 2013) as a reliable estimate of near-peak to early retrograde, regional high-T metamorphic conditions in the Mikawa area.

Gneissose granitoids exposed in the southern, high-grade part of the Mikawa area have long been considered as the heat source of regional high-T metamorphic conditions (e.g. Harayama et al., 1985). However, the southern gneissose granitoids yield U−Pb zircon ages of *ca* 81 Ma and 78−77 Ma which are younger than the timing of near-peak, regional high-T metamorphism in the Grt−Crd zone (*ca* 87 Ma; Figure 7). This clear age difference indicates that heat advected by the southern gneissose granitoids did not contribute to the genesis of the regional metamorphic zones, i.e. that these granitoids are not the direct heat source which produced the low dP/dT metamorphic field gradient.

In addition, we report U−Pb zircon ages of gneissose granitoids that are notably older than metamorphic zircon ages in the Grt−Crd zone migmatite (Figure 7). The northern gneissose granitoids document plutonic activity from *ca* 99 Ma to *ca* 95 Ma at a depth which remains unclear. Such intrusions possibly triggered immediate heating of the surrounding rocks (e.g. Okudaira, 1996), which would be in agreement with CHIME monazite ages obtained from the neighboring metasedimentary rocks (*ca* 99 Ma; Suzuki et al., 1994a, 1994b). However, the northern gneissose granitoids occur far from the presently exposed Grt−Crd zone, and are not likely to have provided heat to the Grt−Crd zone. Therefore, they are not considered as a direct heat source for the low d*P*/d*T* metamorphic field gradient increasing toward the south. It is still possible that these granitoids, which preceded the timing of regional high-*T* conditions, indirectly contributed to a thermal maturation of the upper crust, as proposed in the Yanai area (Skrzypek et al., 2016).

Our results highlight that gneissose granitoids from the Ryoke belt can preserve U−Pb zircon ages that are markedly different from the timing of regional high-*T* metamorphism. Notably, some gneissose granitoids classified as "Older Ryoke granitoids" (e.g. Ryoke Research Group, 1972) are younger than regional high-*T* metamorphism. We therefore emphasize that it is misleading to group granitoids or infer their intrusion timing on the sole base of their gneissose structure. It is equally risky to systematically consider the so-called "gneissose granitoids" as the source of regional high-*T* conditions in the Ryoke belt. The absence of granitoids that are contemporaneous with the formation of the highest-grade regional metamorphic zones in the Mikawa area implies that the contribution of heat conduction from below was more important than the heat advection by granite intrusions. Possible causes for a significant heat conduction towards the middle crust are (1) heat advection by mafic magma intrusions into the lower crust by prolonged mafic magma intrusions or (2) asthenospheric mantle upwelling, which remains a problem to be solved.

8 CONCLUSIONS

1. U−Pb zircon ages of *ca* 99 Ma and 95 Ma are obtained from gneissose granitoids in the northern part of the Mikawa area.
2. Gneissose granitoids in the southern part show distinctly younger U−Pb zircon ages (*ca* 81−77 Ma) than the northern ones. This is younger than the timing of regional high-T metamorphism, suggesting that gneissose granitoids are not the direct heat source for the low dP/dT metamorphic field gradient observed in the Mikawa area.

ACKNOWLEDGEMENTS

We are grateful to T. Okudaira and T. Ikeda for helpful reviews and K. Michibayashi and T. Muto for editorial efforts. K. Tani, K. Suzuki and T. Nakajima are thanked for discussions on the granitoids of the Mikawa area. K. Horie, M. Takehara, T. Kogiso, M. Takaya and Y. Monta are thanked for assistance in sample preparation and F. Higashino for U−Pb zircon dating. This study was financially supported by JSPS KAKENHI Grant Number 26400513 and NIPR general collaboration project No. 28−25 to T. Kawakami, and by a JSPS postdoctoral fellowship to E. Skrzypek (Grant No. 25−03715 to T. Hirajima).

REFERENCES

Bosse, V., Boulvais, P., Gautier, P., Tiepolo, M., Ruffet, G., Devidal, J. L., ... Paquette, J. L. (2009). Fluid-induced disturbance of the monazite Th-Pb chronometer: In situ dating and element mapping in pegmatites from the Rhodope (Greece, Bulgaria). *Chemical Geology*, *261*, 286–302.

Brown, M. (1998). Unpairing metamorphic belts: *P-T* paths and a tectonic model for the Ryoke Belt, southwest Japan. *Journal of Metamorphic Geology*, *16*, 3−22.

De Yoreo, J. J., Lux D. R., & Guidotti, C. V. (1991). Thermal modelling in low-pressure/high-temperature metamorphic belts. *Tectonophysics*, *188*, 209−238.

De Yoreo, J. J., Lux D. R., Guidotti, C. V., Decker, E. R., & Osberg, P. H. (1989). The Acadian thermal history of western Maine. *Journal of Metamorphic Geology*, *7*, 169−190.

Endo, S., & Yamasaki, T. (2013). Geology of the Ryoke Plutono-Metamorphic Complex in the Tsukude area, central Japan. *Bulletin of the Geological Survey of Japan*, *64*, 59−84 (in Japanese with English abstract).

Geological Survey of Japan. (2015). Seamless digital geological map of Japan 1: 200,000. May 29, 2015 version. Geological Survey of Japan, National Institute of Advanced Industrial Science and Technology (Ed.).

Goto, A., & Tatsumi, Y. (1994). Quantitative analysis of rock samples by an X-ray fluorescence spectrometer (I). *The Rigaku Journal*, *11*, 40−59.

Harayama, S., Koido, Y., Ishizawa, K., Nakai, Y., & Kutsukake, T. (1985). Cretaceous to Paleogene Magmatism in the Chubu District, Japan. *Earth Science* (*Chikyu Kagaku*), *39*, 345−357 (in Japanese with English abstract).

Hayama, Y., Yamada, T., Ito, M., Kutsukake, T., Masaoka, K., Miyakawa, K., ... Tsumura, Y. (1982). Geology of the Ryoke Belt in the eastern Kinki District, Japan-The phase-divisions and the mutual relations of the granitic rocks-. *Journal of the Geological Society of Japan*, *88*, 451−466 (in Japanese with English abstract).

Higashimoto, S., Nureki, T., Hara, I., Tsukuda, E., & Nakajima, T. (1983). Geology of the Iwakuni district. Quadrangle Series, 1:50,000. Geological Survey of Japan (in Japanese with English abstract).

Iida, K., Iwamori, H., Orihashi, Y., Park, T., Jwa, Y. J., Kwon, S. T., ... Iwano, H. (2015). Tectonic reconstruction of batholith formation based on the spatiotemporal distribution of Cretaceous–Paleogene granitic rocks in southwestern Japan. *Island Arc*, *24*, 205−220.

Ikeda, T. (1998a). Phase equilibria and the pressure-temperature path of the highest-grade Ryoke metamorphic rocks in the Yanai district, SW Japan. *Contributions to Mineralogy and Petrology*, *132*, 321−335.

Ikeda, T. (1998b). Progressive sequence of reactions of the Ryoke metamorphism in the Yanai district, southwest Japan: the formation of cordierite. *Journal of Metamorphic Geology*, *16*, 39−52.

Ikeda, T. (2004). Pressure-temperature conditions of the Ryoke metamorphic rocks in Yanai district, SW Japan. *Contributions to Mineralogy and Petrology*, *146*, 577−589.

Ishihara, S., & Chappell, B. W. (2007). Chemical compositions of the late Cretaceous Ryoke granitoids of the Chubu District, central Japan-Revisited. *Bulletin of the Geological Survey of Japan*, *58*, 323−350.

Ishihara, S., & Terashima, S. (1977). Chemical variation of the Cretaceous granitoids across southwestern Japan -Shirakawa-Toki-Okazaki transection-. *Journal of the Geological Society of Japan*, *83*, 1−18.

Jackson, S.E., Pearson, N.J., Griffin, W.L., & Belousova, E.A. (2004). The application of laser ablation-inductively coupled plasma-mass spectrometry (LA-ICP-MS) to in-situ U–Pb zircon geochronology. *Chemical Geology*, *211*, 47-69.

Jochum, K. P., & Brueckner, S. M. (2008). Reference materials in geoanalytical and environmental research - Review for 2006 and 2007. *Geostandards and Geoanalytical Research*, *32*, 405−452.

Kawakami, T. (2001). Tourmaline breakdown in the migmatite zone of the Ryoke metamorphic belt, SW Japan. *Journal of Metamorphic Geology*, *19*, 61−75.

Kawakami, T., Nakano, N., Higashino, F., Hokada, T., Osanai, Y., Yuhara, M., ... Hirata, T. (2014). U−Pb zircon and CHIME monazite dating of granitoids and high-grade metamorphic rocks from the Eastern and Peninsular Thailand — A new report of Early Paleozoic granite. *Lithos*, *200−201*, 64−79.

Kawakami, T., & Suzuki, K. (2011). CHIME monazite dating as a tool to detect polymetamorphism in high-temperature metamorphic terrane: Example from the Aoyama area, Ryoke metamorphic belt, Southwest Japan. *Island Arc*, *20*, 439−453.

Kawakami, T., Yamaguchi, I., Miyake, A., Shibata, T., Maki, K., Yokoyama, T. D. & Hirata, T. (2013). Behavior of zircon in the upper-amphibolite to granulite facies schist/migmatite transition, Ryoke metamorphic belt, SW Japan: constraints from the melt inclusions in zircon. *Contributions to Mineralogy and Petrology*, *165*, 575−591.

Koide, H. (1942). On the granitic rocks of the Tenryukyo district, Nagano Prefecture, Japan. *Bulletin of Tokyo Imperial University Forest*, *30*, 69−95 (in Japanese with English abstract).

Kretz, R. (1983). Symbols for rock-forming minerals. *American Mineralogist*, *68*, 277−279.

Kutsukake, T. (1993). An initial continental margin plutonism-Cretaceous Older Ryoke granitoids, southwest Japan. *Geological Magazine*, *130*, 15−28.

Kutsukake, T. (1997). Petrology and geochemistry of a calcic and ferrous granitoid pluton: the Mitsuhashi Granite in the Ryoke Belt, southwest Japan. *Journal of Mineralogy, Petrology and Economic Geology*, *92*, 231−244.

Kutsukake, T. (2001). Geochemistry of the Kiyosaki Granodiorite in the Ryoke Belt, central Japan. *Science Report of the Toyohashi Museum of Natural History*, *11*, 1−12.

Ludwig, K. (2012). User's manual for Isoplot version 3.75−4.15: a geochronological toolkit for Microsoft Excel. *Berkley Geochronological Center Special Publication 5*.

Lux, D. R., De Yoreo, J. J., Guldotti, C. V., & Decker, E. R. (1986). Role of plutonism in low-pressure metamorphic belt formation. *Nature*, *323*, 794−797.

Makimoto, H., Yamada, N., Mizuno, K., Takada, A., Komazawa, M., & Sudo, S. (2004). Geological map of Japan 1: 200,000, Toyohashi and Irago Misaki. Geological Survey of Japan (in Japanese with English abstract).

Masumoto, Y., Enami, M., Tsuboi, M., & Hong, M. (2014). Magmatic zoisite and epidote in tonalite of the Ryoke belt, central Japan. *European Journal of Mineralogy*, *26*, 279−291.

Miyake, A., Hirukawa, T., Sato, M., Taguchi, T., Suzuki, K., & Nakai, Y. (2016). Large thermal aureole around the Inagawa Granodiorite in the southeastern area of Asuke, Aichi Prefecture. *Journal of the Geological Society of Japan*, *122*, 173−191 (in Japanese with English abstract).

Miyashiro, A. (1961). Evolution of metamorphic belts. *Journal of Petrology*, *2*, 277−311.

Miyazaki, K. (2010). Development of migmatites and the role of viscous segregation in high-T metamorphic complexes: Example from the Ryoke Metamorphic Complex, Mikawa Plateau, Central Japan. *Lithos*, *116*, 287−299.

Miyazaki, K., Nishioka, Y., Nakashima, R., & Ozaki, M. (2008). Geology of the Goyu district. Quadrangle Series, 1:50,000. Geological Survey of Japan (in Japanese with English abstract).

Morishita, T., & Suzuki, K. (1993). XRF analyses of the Mitsuhashi Granite in the Shitara area, Aichi Prefecture. *Bulletin of the Nagoya University Furukawa Museum*, *9*, 77−90 (in Japanese with English abstract).

Morishita, T., & Suzuki, K. (1995). CHIME ages of monazite from the Shinshiro Tonalite of the Ryoke belt in the Mikawa area, Aichi Prefecture. *The Journal of Earth and Planetary Sciences, Nagoya University*, *42*, 45−53.

Morishita, T., Suzuki, K., & Nasu, T. (1996). CHIME ages of monazite from granitoids in the Mikawa-Tono area, central Japan. *The 103rd Annual Meeting of the Geological Society of Japan*, *Abstracts*, *282* (in Japanese).

Murakami, M., Košler, J., Takagi, H., & Tagami, T. (2006). Dating pseudotachylyte of the Asuke Shear Zone using zircon fission-track and U−Pb methods. *Tectonophysics*, *424*, 99−107.

Nakai, Y. (1974). Compositional variations of the Inagawa granitic rocks in the Asuke area, Aichi prefecture, central Japan. *The Journal of the Japanese Association of Mineralogists, Petrologists and Economic Geologists*, *69*, 215−224.

Nakai, Y. (1976). Petrographical and petrochemical studies of the Ryoke granites in the Mikawa-Tono district, central Japan. *Bulletin of Aichi University of Education* (*Natural Science*), *25*, 97−112.

Nakai, Y., & Suzuki, K. (1996). CHIME monazite ages of the Kamihara Tonalite and the Tenryukyo Granodiorite in the eastern Ryoke belt of central Japan. *Journal of the Geological Society of Japan*, *102*, 431−439.

Nakai, Y., & Suzuki, K. (2003). Post-tectonic two-mica granite in the Okazaki area, central Japan: a field guide for the 2003 Hutton Symposium. Hutton Symposium, V, Field Guidebook, Geological Survey of Japan, Interim-Report, 28, 115−124.

Nakajima, T. (1994). The Ryoke plutonometamorphic belt: crustal section of the Cretaceous Eurasian continental margin. *Lithos*, *33*, 51−66.

Nakajima, T. (1996). Cretaceous granitoids in SW Japan and their bearing on the crust-forming process in the eastern Eurasian margin. *Transactions of the Royal Society of Edinburgh: Earth Science*, *87*, 183−191.

Nakajima, T., Horie, K., Adachi, T., Miyazaki, K., Dunkley, D. J., & Hokada, T. (2013). SHRIMP U−Pb ages of zircons from Ryoke metamorphic rocks. *The 120th Annual Meeting of the Geological Society of Japan, Abstracts*, *51* (in Japanese).

Nakajima, T., Kamiyama, H., Williams, I. S., & Tani, K. (2004). Mafic rocks from the Ryoke Belt, southwest Japan: implications for Cretaceous Ryoke/San-yo granitic magma genesis. *Geological Society of America Special Papers*, *389*, 249−263.

Nakashima, R., Hori, N., Miyazaki, K., & Nishioka, Y. (2008). Geology of the Toyohashi and Tahara districts. Quadrangle Series, 1:50,000. Geological Survey of Japan (in Japanese with English abstract).

Ohtomo, Y. (1985). Zonal structure of the Shinshiro Tonalite pluton. *MAGMA*, *73*, 69−73 (in Japanese).

Okudaira, T. (1996). Thermal evolution of the Ryoke metamorphic belt, southwestern Japan: tectonic and numerical modeling. *Island Arc*, *5*, 373−385.

Okudaira, T., Hara, I., Sakurai, Y., & Hayasaka, Y. (1993). Tectono-metamorphic processes of the Ryoke belt in the Iwakuni-Yanai district, southwest Japan. *Memoirs of the Geological Society of Japan*, *42*, 91−120.

Okudaira, T., & Suda, Y. (2011). Cretaceous events at the eastern margin of East Asia recorded in rocks of the Ryoke belt, SW Japan. *Journal of Geography*, *120*, 452−465 (in Japanese with English abstract).

Pearce, N. J., Perkins, W. T., Westgate, J. A., Gorton, M. P., Jackson, S. E., Neal, C. R., & Chenery, S. P. (1997). A compilation of new and published major and trace element data for NIST SRM 610 and NIST SRM 612 glass reference materials. *Geostandards Newsletter*, *21*, 115−144.

Poitrasson, F., Chenery, S., & Bland, D. J. (1996). Contrasted monazite hydrothermal alteration mechanisms and their geochemical implications. *Earth and Planetary*

Science Letters, *145*, 79–96.

Ryoke Research Group. (1972). The mutual relations of the granitic rocks of the Ryoke metamorphic belt in central Japan. *Earth Science* (*Chikyu Kagaku*), *26*, 205−216 (in Japanese with English abstract).

Sakakibara, Y. (1967). Fore Ryoke granitic rocks of the Niino district, Shimoina, Nagano Prefecture. Professor Hidekata Shibata Memorial Volume, 63−71 (in Japanese with English abstract).

Skrzypek, E., Kawakami, T., Hirajima, T., Sakata, S., Hirata, T., & Ikeda, T. (2016). Revisiting the high temperature metamorphic field gradient of the Ryoke Belt (SW Japan): New constraints from the Iwakuni-Yanai area. *Lithos*, *260*, 9−27.

Sláma, J., Košler, J., Condon, D. J., Crowley, J. L., Gerdes, A., Hanchar, J. M., ... Whitehouse, M. J. (2008). Plešovice zircon — A new natural reference material for U–Pb and Hf isotopic microanalysis. *Chemical Geology*, *249*, 1−35.

Suzuki, K., & Adachi, M. (1998). Denudation history of the high T/P Ryoke metamorphic belt, southwest Japan: constraints from CHIME monazite ages of gneisses and granitoids. *Journal of Metamorphic Geology*, *16*, 23−37.

Suzuki, K., Adachi, M., & Kajizuka, I. (1994a). Electron microprobe observations of Pb diffusion in metamorphosed detrital monazites. *Earth and Planetary Science Letters*, *128*, 391−405.

Suzuki, K., Morishita, T., Kajizuka, I., Nakai, Y., Adachi, M., & Shibata, K. (1994b). CHIME ages of monazites from the Ryoke metamorphic rocks and some granitoids in the Mikawa-Tono area, central Japan. *Bulletin of the Nagoya University Furukawa Museum*, *10*, 7−38 (in Japanese with English abstract).

Tani, K., Horie, K., Dunkley, D., & Ishihara, S. (2014). Pulsed granitic crust formation revealed by comprehensive SHRIMP zircon dating of the SW Japan granitoids. *Abstract of the Japan Geoscience Union Meeting 2014,* SCG61-01.

Tsuboi, M., & Asahara, Y. (2009). Initial $^{87}Sr/^{86}Sr$ ratio heterogeneity in Kamihara Tonalite, Ryoke belt, southwest Japan: Evidence from strontium isotopic analysis of apatite. *Journal of Mineralogical and Petrological Sciences*, *104*, 226−233.

Wakita, K. (1987). The occurrence of Latest Jurassic-Earliest Cretaceous radiolarians at the Hida-Kanayama area in the Mino terrane, central Japan. *Journal of the Geological Society of Japan*, *93*, 441−443 (in Japanese).

Watanabe, T., Ireland, T., Tainosho, Y., & Nakai, Y. (2000). Zircon U–Pb sensitive high mass-resolution ion microprobe dating of granitoids in the Ryoke metamorphic belt, Kinki District, Southwest Japan. *Island Arc*, *9*, 55−63.

Wayne, D. M., & Sinha, A. K. (1988). Physical and chemical response of zircons to deformation. *Contributions to Mineralogy and Petrology*, *98*, 109−121.

Wiedenbeck, M., Alle, P., Corfu, F., Griffin, W. L., Meier, M., Oberli, F., ... Spiegel, W. (1995). Three natural zircon standards for U−Th−Pb, Lu−Hf, trace element and REE analyses. *Geostandards Newsletter*, *19*, 1−23.

Wiedenbeck, M., Hanchar, J. M., Peck, W. H., Sylvester, P., Valley, J., Whitehouse, M., ... Zheng, Y. -F. (2004). Further characterisation of the 91500 zircon crystal. *Geostandards and Geoanalytical Research*, *28*, 9−39.

Yamasaki, T. (2013). K−Ar ages of the Ryoke plutonic rocks in the Asuke area, Aichi prefecture, central Japan. *Journal of the Geological Society of Japan*, *119*, 421−431 (in Japanese with English abstract).

Yamasaki, T., & Ozaki, M. (2012). Geology of the Asuke district. Quadrangle Series, 1:50,000. Geological Survey of Japan (in Japanese with English abstract).

LIST OF SUPPORTING INFORMATION

Table S1. Summary of analytical procedures and data reduction scheme for LA-ICP-MS U−Pb zircon dating.

Table S2. Summary of LA-ICP-MS U−Pb zircon analyses.

FIGURE CAPTIONS

FIGURE 1. Geological map of the Ryoke belt in central Japan (Mikawa and Toyone areas). Inset shows the distribution of the Ryoke belt across Japan and the locations of the study area and the Yanai and Aoyama areas. The sampling localities of gneissose granitoids are indicated. Mineral abbreviations are after Kretz (1983). Compiled and modified after Endo and Yamasaki (2013), Makimoto et al. (2004), Miyazaki (2010), and the Geological Survey of Japan (2015). MTL, Median Tectonic Line; ISTL, Itoigawa–Shizuoka Tectonic Line. Metamorphic zones in the Mikawa area are after Endo and Yamasaki (2013), Miyazaki et al. (2008), Nakashima et al. (2008), and Yamasaki & Ozaki (2012).

FIGURE 2. Slab photographs and photomicrographs (open nicol) of gneissose granitoids collected from northern Mikawa. (a–d) Samples GY88A and GY90A showing a gneissose structure defined by the arrangement of biotite and hornblende. Allanite is present in sample GY90A. (e, f) Sample GY98A showing a weak gneissose structure. Clinopyroxene is partly replaced by hornblende.

FIGURE 3. Field occurrences, slab photographs and photomicrographs (open nicol) of samples collected from southern Mikawa. (a)–(e) Samples GY33A and GY48D from southeast Mikawa: (a) K-feldspar megacrysts up to 3 cm in length arranged parallel to the gneissose structure, (b,d) gneissose structure defined by arrangement of biotite, (c,e) gneissose structure defined by biotite-rich layers. (f)–(j) Samples GY80D and GY81B from southwest Mikawa, (f) gneissose tonalite discordantly cut by fine-grained gabbro (gray), (g) gneissose structure defined by the alternation of leucocratic and melanocratic Hbl－Bt layers, (i) Hbl－Bt clot with zircon inclusions in biotite, (h, j) gneissose structure defined by the alternation of leucocratic and melanocratic Hbl－Bt layers.

FIGURE 4. Selected Harker diagrams for gneissose granitoids from the Mikawa and Toyone areas. The composition of the studied samples is plotted together with published data from Ishihara and Chappell (2007), Ishihara and Terashima (1977), Kutsukake (1993), Masumoto et al. (2014), Morishita and Suzuki (1993), Nakai (1976), Tsuboi and Asahara (2009), and Yamasaki (2013). See text for detailed discussion.

FIGURE 5. Cathodoluminescence images of representative zircon grains with analyzed spots and results of U–Pb dating. Results are labeled with spot number, $^{206}Pb/^{238}U$ age

±2σ error (Ma), and concordance in parentheses (%). Results shown in yellow denote concordant data, whereas those shown in white with asterisk denote discordant data. Scale bars represent 20 μm.

FIGURE 6. Concordia diagrams of U−Pb zircon data. (a)−(c) Samples from northern Mikawa. (d)−(e) Samples from southeast Mikawa. (f, g) southwest Mikawa. Concordant and discordant data are plotted with filled and open ellipses, respectively. Rejected data (see Table S2) are not shown. The weighted mean $^{206}Pb/^{238}U$ ages ±2σ error (Ma) are shown together with the number of concordant data used for calculation (*n*) and the associated mean square of weighted deviates (MSWD).

FIGURE 7. Summary of U−Pb zircon ages (This study; Tani et al., 2014; Nakajima et al., 2013) and CHIME monazite ages (Nakai & Suzuki, 1996; Suzuki & Adachi, 1998; Suzuki et al., 1994a, 1994b) from the Mikawa and Toyone areas. $^{206}Pb/^{238}U$ zircon ages are shown with 2σ uncertainties.

FIGURE 8. Summary of U−Pb zircon dating and tentative correlations between gneissose granitoids in the Mikawa and Toyone areas. $^{206}Pb/^{238}U$ zircon ages are shown

with 2σ uncertainties. See text for detailed discussion.

Table 1. Bulk-rock analyses of samples from the Mikawa area selected for U−Pb zircon dating.

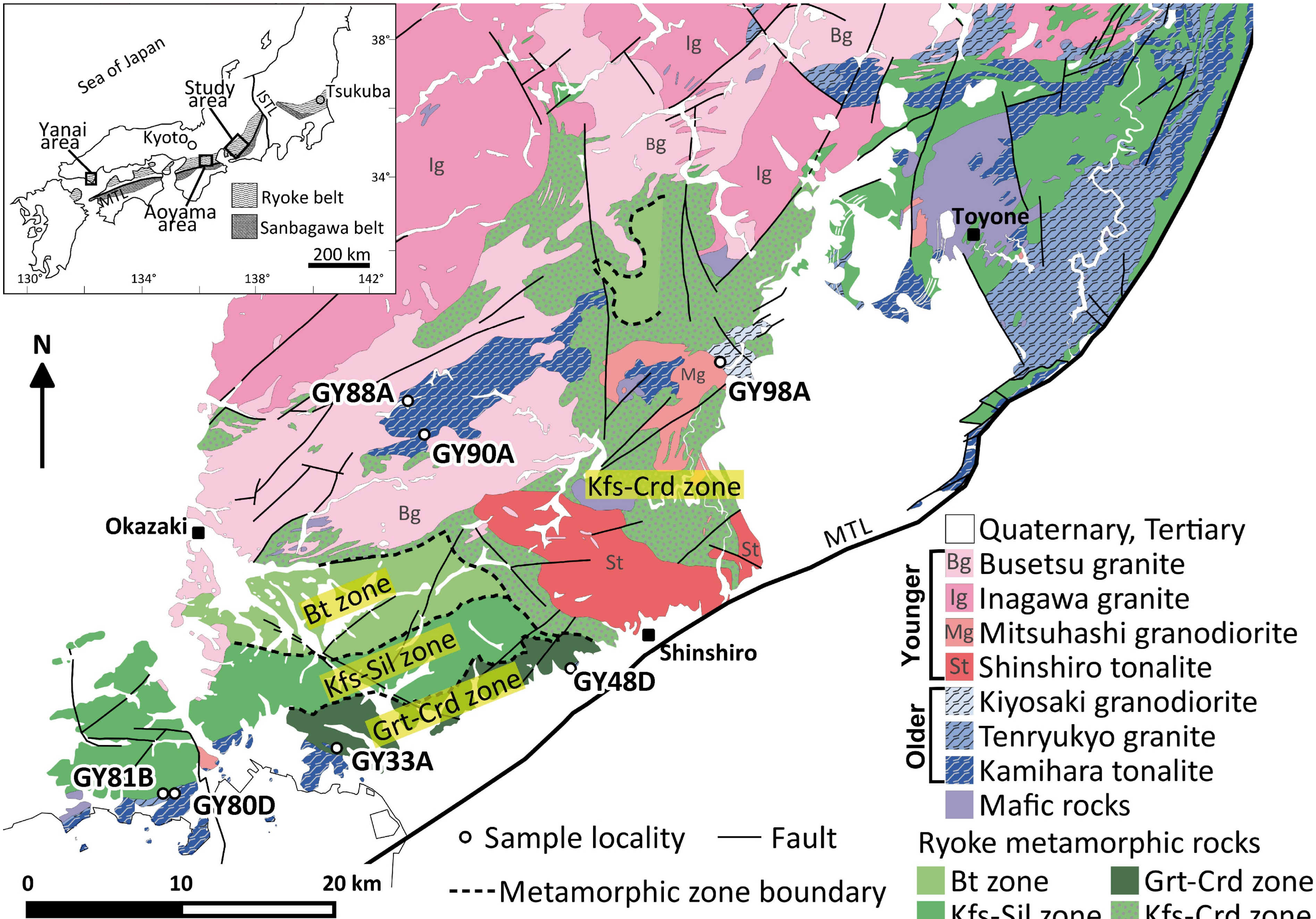

Sea of Japan
Study area
ISTL
Tsukuba
Yanai area
Kyoto
MTL
Aoyama area
Ryoke belt
Sanbagawa belt
200 km
38°
34°
130°
134°
138°
142°
N
Ig
Bg
Mg
St
GY88A
GY90A
GY98A
Toyone
Kfs-Crd zone
Okazaki
Bt zone
Kfs-Sil zone
Grt-Crd zone
Shinshiro
GY48D
GY33A
GY81B
GY80D
MTL
0
10
20 km
Sample locality
Fault
Metamorphic zone boundary
Quaternary, Tertiary
Younger
Bg Busetsu granite
Ig Inagawa granite
Mg Mitsuhashi granodiorite
St Shinshiro tonalite
Older
Kiyosaki granodiorite
Tenryukyo granite
Kamihara tonalite
Mafic rocks
Ryoke metamorphic rocks
Bt zone
Kfs-Sil zone
Grt-Crd zone
Kfs-Crd zone

===================== Northern Mikawa =====================

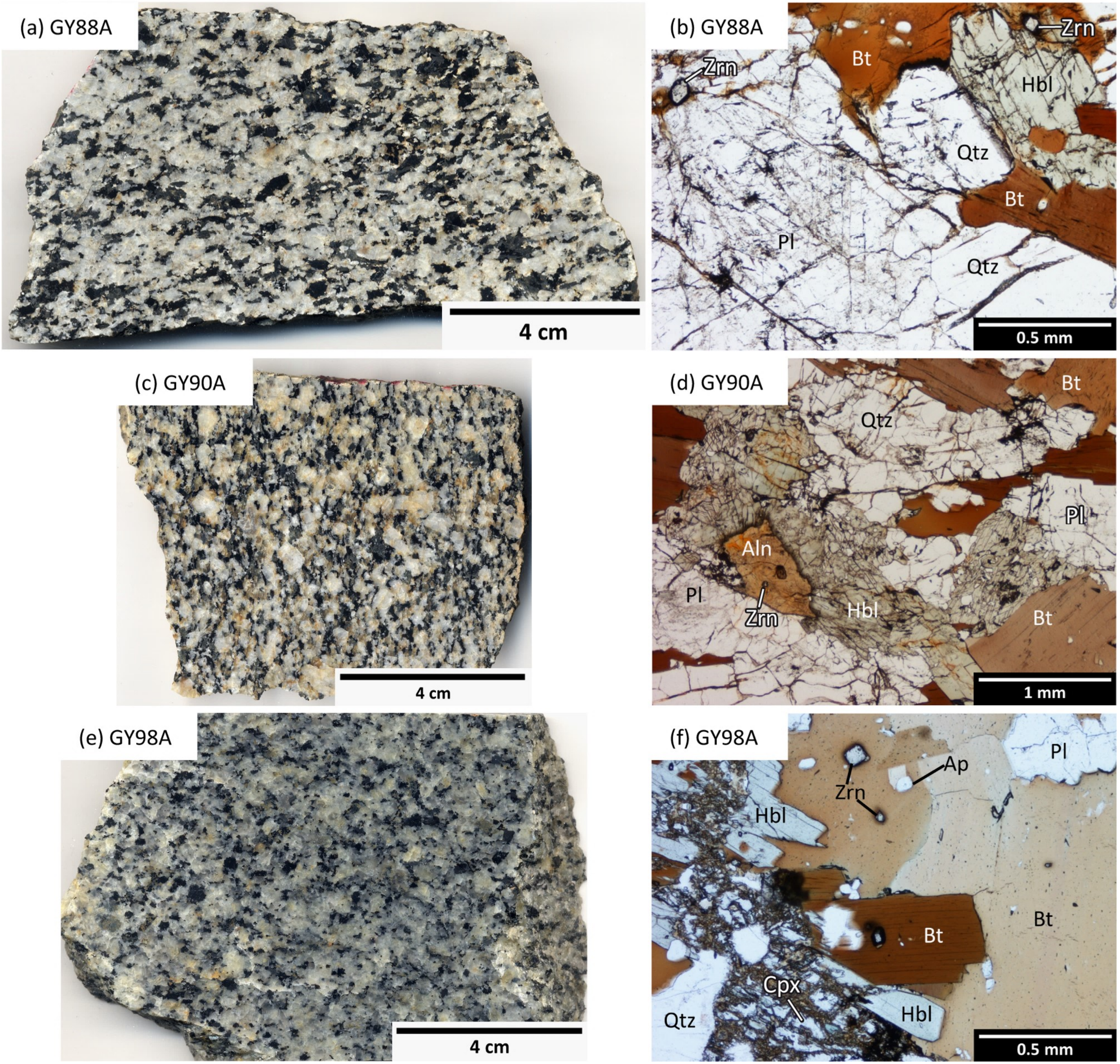

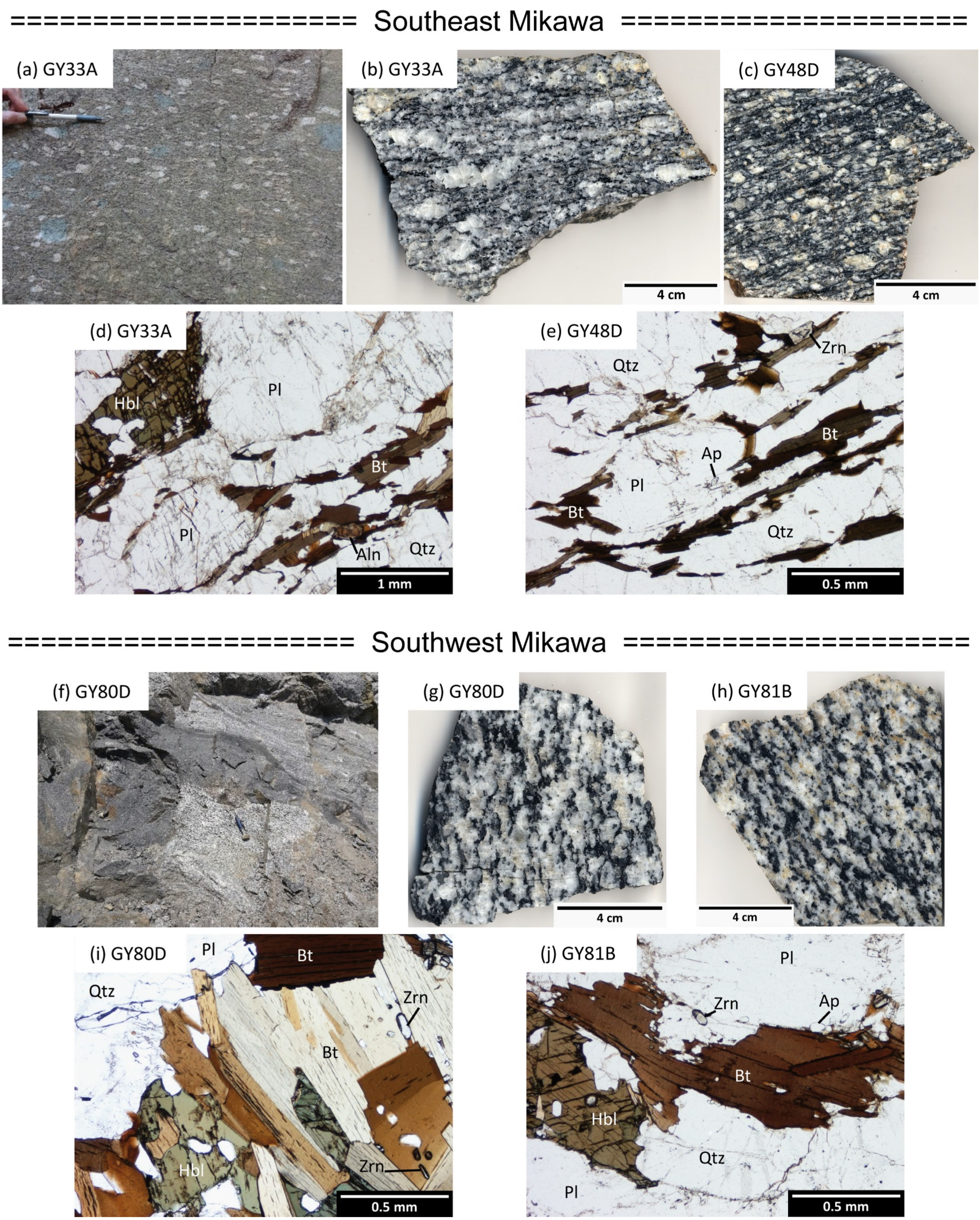

Southeast Mikawa
(a) GY33A
(b) GY33A
4 cm
(c) GY48D
4 cm
(d) GY33A
Hbl
Pl
Bt
Pl
Aln
Qtz
1 mm
(e) GY48D
Zrn
Qtz
Bt
Ap
Pl
Bt
Qtz
0.5 mm
Southwest Mikawa
(f) GY80D
(g) GY80D
4 cm
(h) GY81B
4 cm
(i) GY80D
Pl
Bt
Qtz
Zrn
Bt
Hbl
Zrn
0.5 mm
(j) GY81B
Pl
Zrn
Ap
Bt
Hbl
Qtz
Pl
0.5 mm

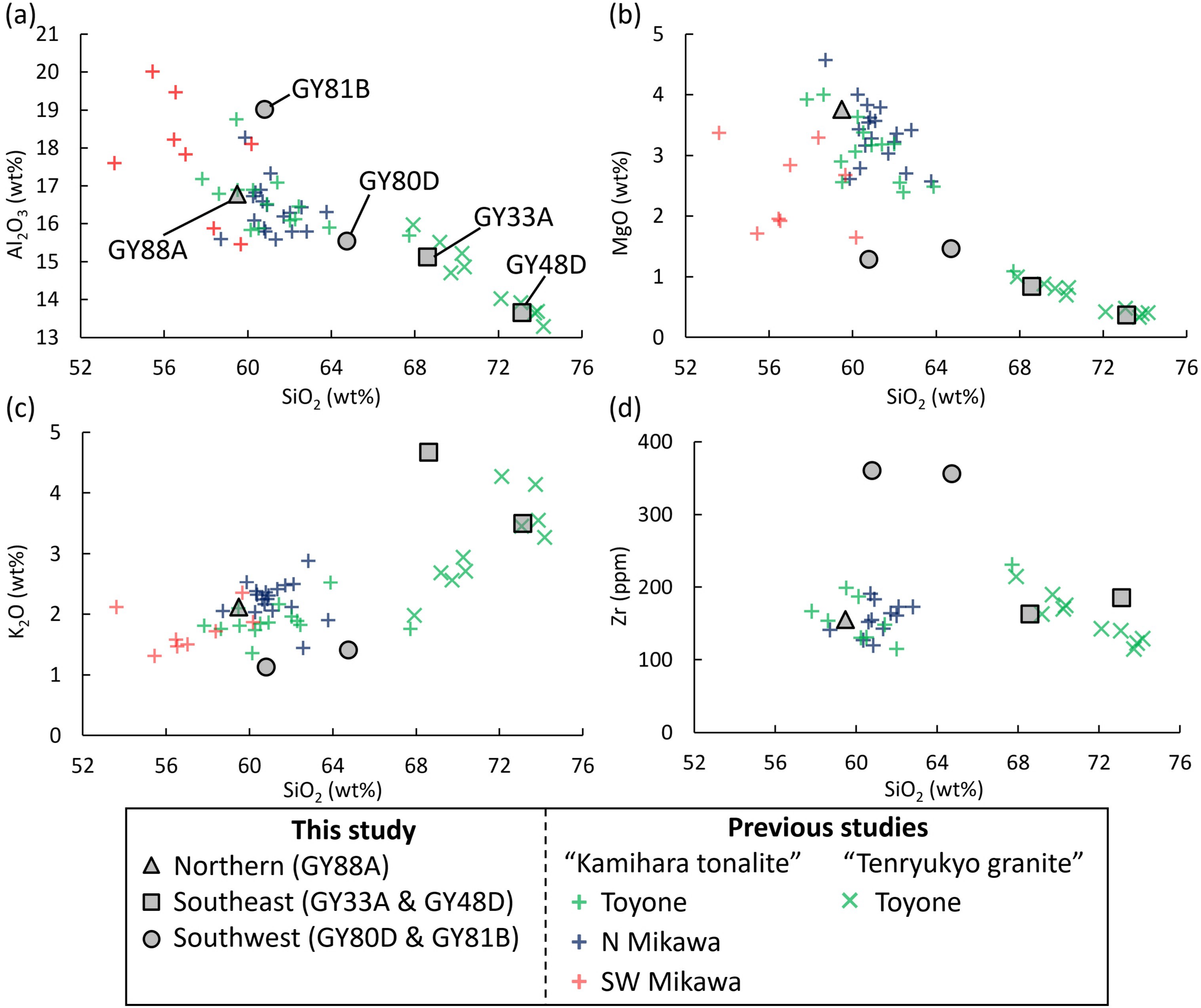
(a)
GY81B
GY80D
GY33A
GY88A
GY48D
Al_2O_3 (wt%)
SiO_2 (wt%)
(b)
MgO (wt%)
SiO_2 (wt%)
(c)
K_2O (wt%)
SiO_2 (wt%)
(d)
Zr (ppm)
SiO_2 (wt%)
This study
Northern (GY88A)
Southeast (GY33A & GY48D)
Southwest (GY80D & GY81B)
Previous studies
"Kamihara tonalite"
Toyone
N Mikawa
SW Mikawa
"Tenryukyo granite"
Toyone

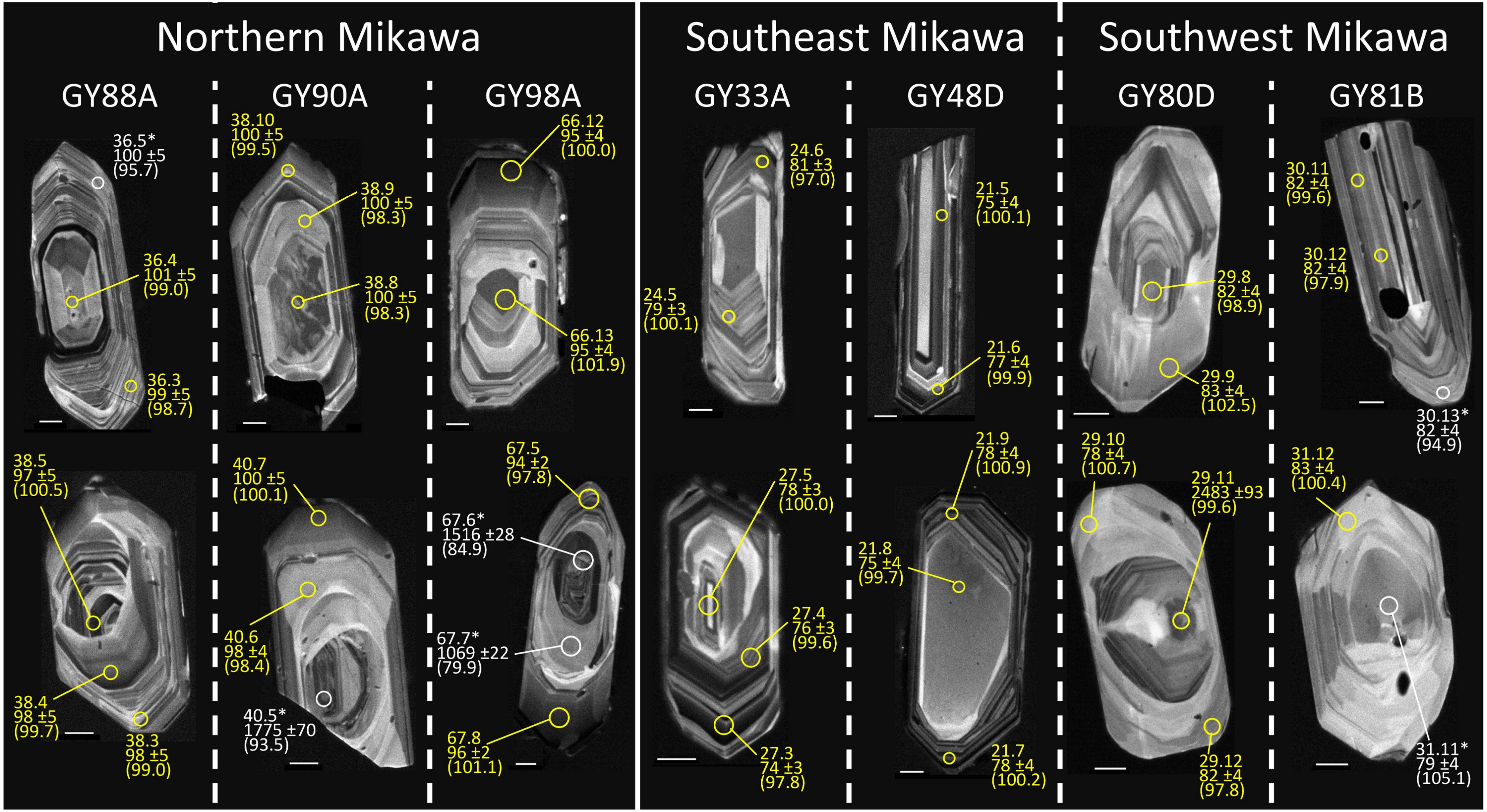

Northern Mikawa
Southeast Mikawa
Southwest Mikawa
GY88A
GY90A
GY98A
GY33A
GY48D
GY80D
GY81B
36.5* 100 ±5 (95.7)
36.4 101 ±5 (99.0)
36.3 99 ±5 (98.7)
38.10 100 ±5 (99.5)
38.9 100 ±5 (98.3)
38.8 100 ±5 (98.3)
66.12 95 ±4 (100.0)
66.13 95 ±4 (101.9)
24.6 81 ±3 (97.0)
24.5 79 ±3 (100.1)
21.5 75 ±4 (100.1)
21.6 77 ±4 (99.9)
29.8 82 ±4 (98.9)
29.9 83 ±4 (102.5)
30.11 82 ±4 (99.6)
30.12 82 ±4 (97.9)
30.13* 82 ±4 (94.9)
38.5 97 ±5 (100.5)
38.4 98 ±5 (99.7)
38.3 98 ±5 (99.0)
40.7 100 ±5 (100.1)
40.6 98 ±4 (98.4)
40.5* 1775 ±70 (93.5)
67.5 94 ±2 (97.8)
67.6* 1516 ±28 (84.9)
67.7* 1069 ±22 (79.9)
67.8 96 ±2 (101.1)
27.5 78 ±3 (100.0)
27.4 76 ±3 (99.6)
27.3 74 ±3 (97.8)
21.9 78 ±4 (100.9)
21.8 75 ±4 (99.7)
21.7 78 ±4 (100.2)
29.10 78 ±4 (100.7)
29.11 2483 ±93 (99.6)
29.12 82 ±4 (97.8)
31.12 83 ±4 (100.4)
31.11* 79 ±4 (105.1)

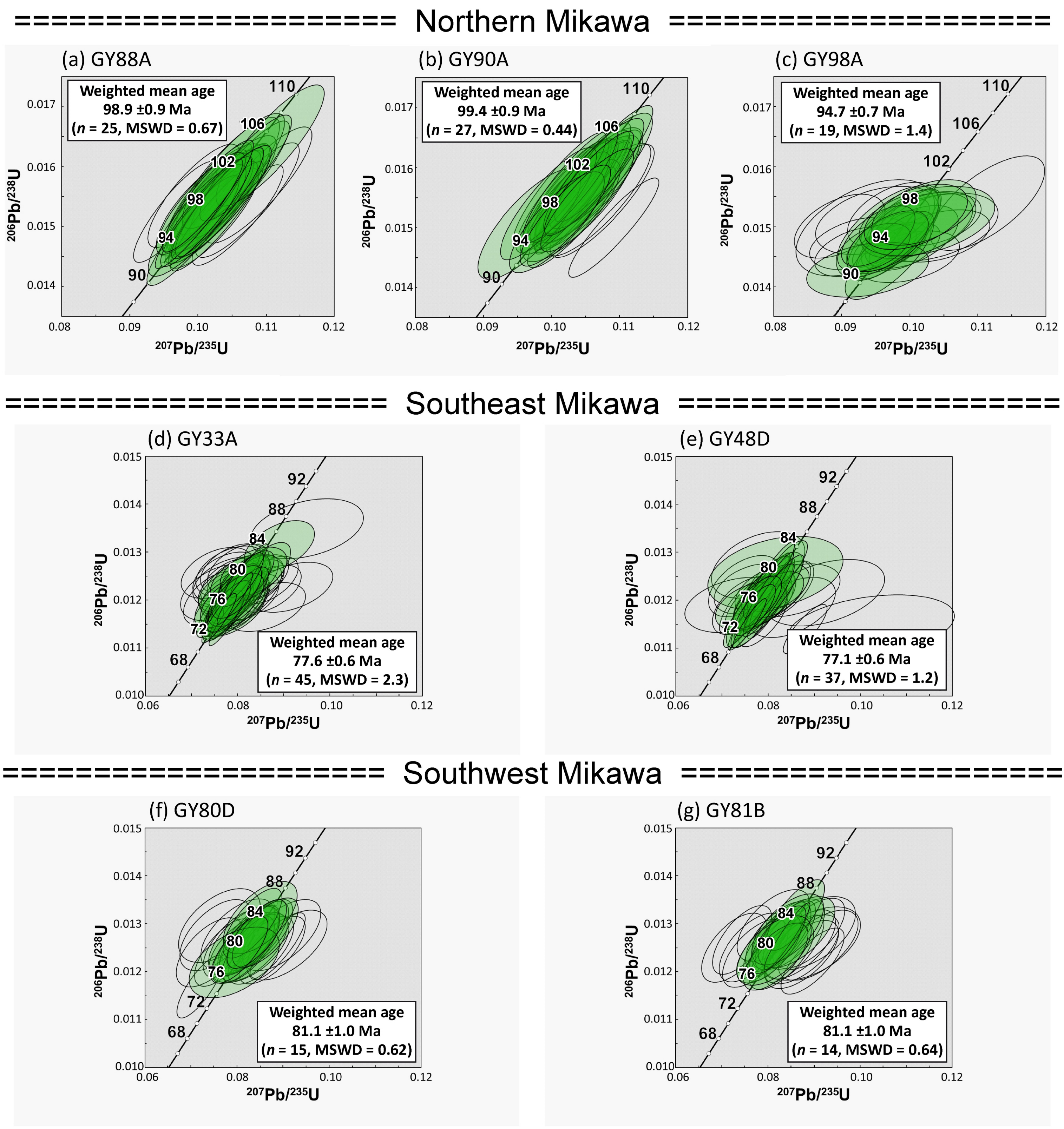

Northern Mikawa
(a) GY88A
Weighted mean age
98.9 ±0.9 Ma
(n = 25, MSWD = 0.67)
(b) GY90A
Weighted mean age
99.4 ±0.9 Ma
(n = 27, MSWD = 0.44)
(c) GY98A
Weighted mean age
94.7 ±0.7 Ma
(n = 19, MSWD = 1.4)
Southeast Mikawa
(d) GY33A
Weighted mean age
77.6 ±0.6 Ma
(n = 45, MSWD = 2.3)
(e) GY48D
Weighted mean age
77.1 ±0.6 Ma
(n = 37, MSWD = 1.2)
Southwest Mikawa
(f) GY80D
Weighted mean age
81.1 ±1.0 Ma
(n = 15, MSWD = 0.62)
(g) GY81B
Weighted mean age
81.1 ±1.0 Ma
(n = 14, MSWD = 0.64)
206Pb/238U
207Pb/235U

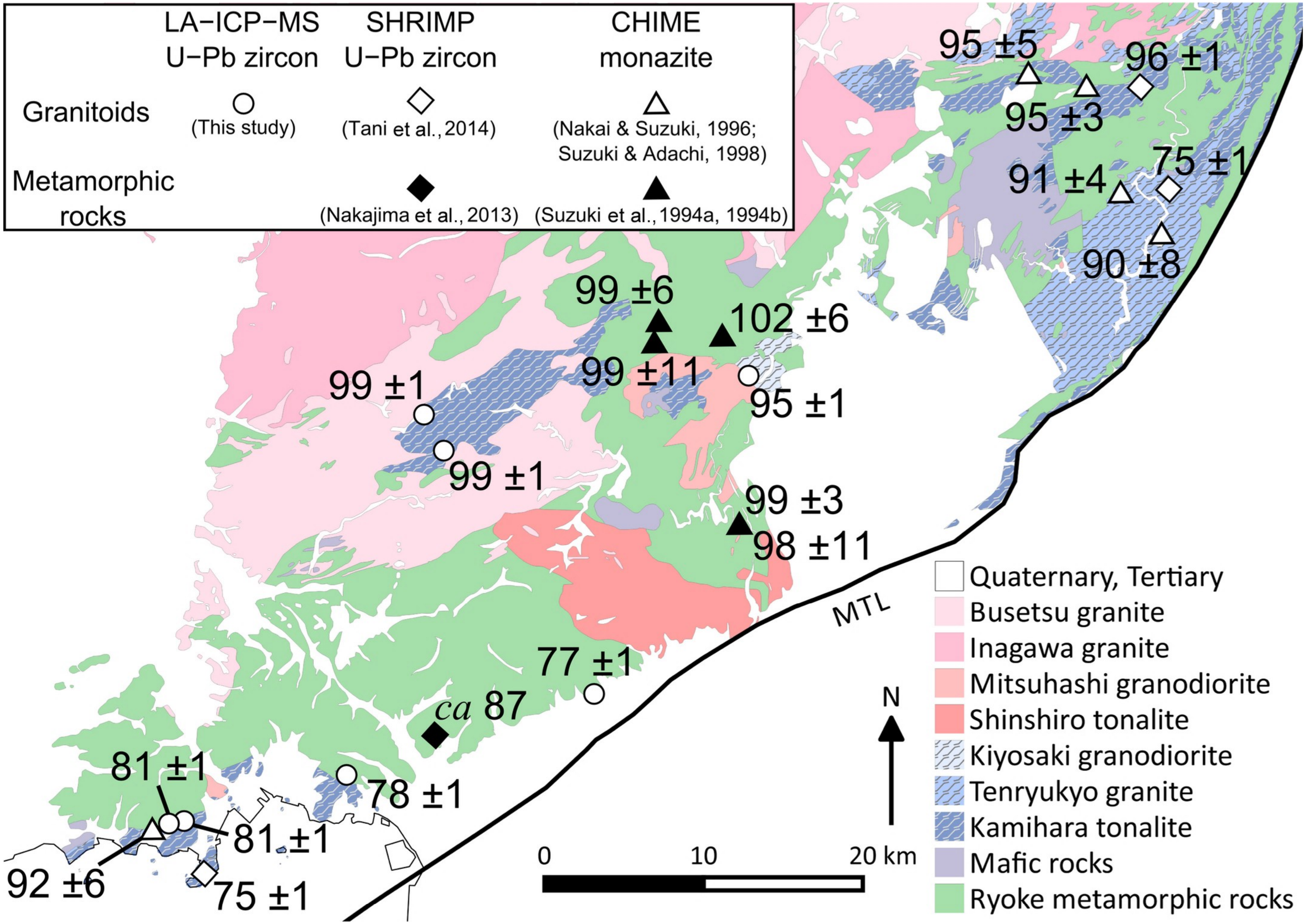
LA−ICP−MS U−Pb zircon
SHRIMP U−Pb zircon
CHIME monazite
Granitoids
(This study)
(Tani et al., 2014)
(Nakai & Suzuki, 1996; Suzuki & Adachi, 1998)
Metamorphic rocks
(Nakajima et al., 2013)
(Suzuki et al., 1994a, 1994b)
95 ±5
96 ±1
95 ±3
75 ±1
91 ±4
90 ±8
99 ±6
102 ±6
99 ±11
95 ±1
99 ±1
99 ±1
99 ±3
98 ±11
MTL
77 ±1
ca 87
81 ±1
78 ±1
81 ±1
92 ±6
75 ±1
N
0
10
20 km
Quaternary, Tertiary
Busetsu granite
Inagawa granite
Mitsuhashi granodiorite
Shinshiro tonalite
Kiyosaki granodiorite
Tenryukyo granite
Kamihara tonalite
Mafic rocks
Ryoke metamorphic rocks

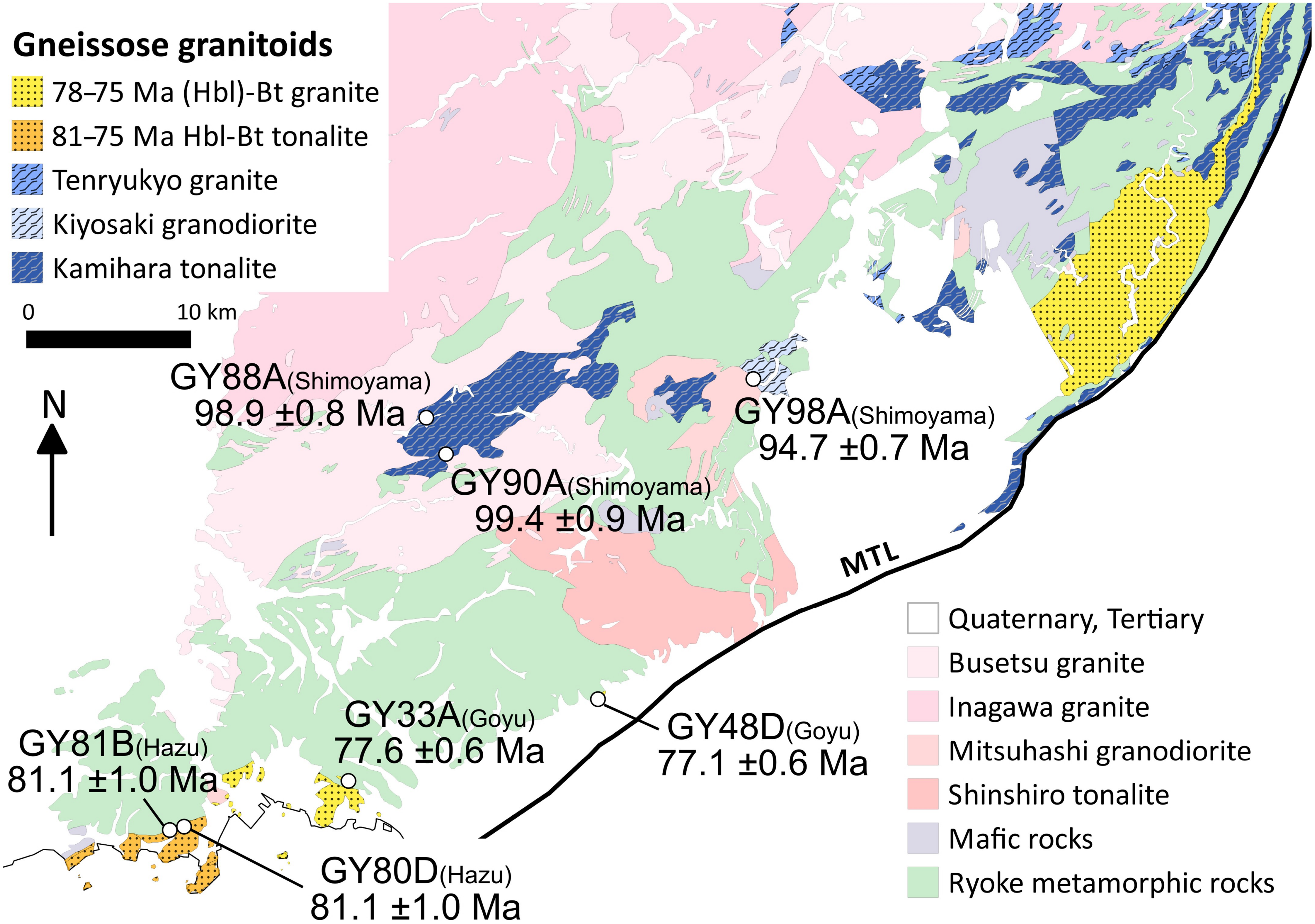
Gneissose granitoids
78–75 Ma (Hbl)-Bt granite
81–75 Ma Hbl-Bt tonalite
Tenryukyo granite
Kiyosaki granodiorite
Kamihara tonalite
0
10 km
N
GY88A(Shimoyama)
98.9 ±0.8 Ma
GY98A(Shimoyama)
94.7 ±0.7 Ma
GY90A(Shimoyama)
99.4 ±0.9 Ma
MTL
GY33A(Goyu)
77.6 ±0.6 Ma
GY48D(Goyu)
77.1 ±0.6 Ma
GY81B(Hazu)
81.1 ±1.0 Ma
GY80D(Hazu)
81.1 ±1.0 Ma
Quaternary, Tertiary
Busetsu granite
Inagawa granite
Mitsuhashi granodiorite
Shinshiro tonalite
Mafic rocks
Ryoke metamorphic rocks

Area	Northern Mikawa	Southeast Mikawa		Southwest Mikawa	
Sample	GY88A	GY33A	GY48D	GY80D	GY81B
SiO_2 (wt%)	59.47	68.58	73.12	64.72	60.78
TiO_2	0.80	0.38	0.23	0.72	0.64
Al_2O_3	16.79	15.13	13.66	15.55	19.03
Fe_2O_3†	6.56	3.40	2.36	6.43	5.17
MnO	0.11	0.06	0.05	0.12	0.09
MgO	3.77	0.84	0.37	1.47	1.29
CaO	5.45	2.79	1.89	4.82	6.29
Na_2O	3.06	2.74	3.50	3.36	3.92
K_2O	2.12	4.67	3.50	1.41	1.13
P_2O_5	0.16	0.08	0.05	0.18	0.17
Cr_2O_3	0.014	b.d.	b.d.	b.d.	b.d.
LOI	1.4	0.9	1.0	0.9	1.2
Total	99.69	99.59	99.75	99.68	99.69
Co (ppm)	118.9	92.0	101.7	74.6	67.6
Ni	26.2	4.6	4.0	6.9	6.1
Zn	56	49	51	77	61
Rb	77.3	84.7	110.4	35.8	26.2
Sr	296.0	313.8	166.8	423.2	584.8
Y	21.0	24.6	15.7	15.8	16.6
Zr	155.3	163.2	185.3	356.1	360.8
Nb	10.9	7.2	9.2	9.3	8.6
Ba	397	1820	586	776	543
Th	3.1	8.9	13.5	3.3	6.0
La	12.5	35.5	35.1	23.1	37.0
Ce	27.6	76.8	71.1	48.8	76.3
Pr	3.92	8.25	7.31	5.51	7.88
Nd	17.7	30.9	27.3	24.0	29.3
Sm	4.04	6.30	4.66	4.98	4.96
Eu	1.00	1.14	0.79	1.65	1.92
Gd	4.31	5.81	3.76	4.79	4.19
Tb	0.69	0.90	0.54	0.66	0.57
Dy	3.91	4.90	2.71	4.03	3.10
Ho	0.79	0.97	0.57	0.66	0.65
Er	2.25	2.62	1.58	1.88	1.80
Tm	0.30	0.37	0.23	0.24	0.25
Yb	1.93	2.19	1.81	1.58	1.67
Lu	0.29	0.33	0.27	0.23	0.29

†Total iron as Fe_2O_3.

b.d., below detection limit.